GAS Journal of Engineering and Technology (GASJET)

Volume 2 | Issue 12, 2025 Homepage: https://gaspublishers.com/gasjet-home/ ISSN: 3048-5800

Effect of Magnetic Field on the Propagation Characteristics of EM Waves in Plasma Filaments Layer with a Three-Layer Circular Structure

Un-Ha Kim, In-Ho Pak, Su-Hyang Pak & Yong-Jun Kim

Faculty of Physical Engineering, Kim Chaek University of Technology, Pyongyang 999093, Democratic People's Republic of Korea

Received: *01.12.2025* | ***Accepted:*** *04.12.2025* | ***Published:*** *17.12.2025*

***Corresponding Author:** Yong-Jun Kim

DOI: *10.5281/zenodo.17966983*

Abstract **Original Research Article**

The effect of magnetic field on the propagation characteristics of electromagnetic (EM) waves in a plasma filaments layer with a three-layer circular structure generated by femtosecond laser was studied. To simulate the propagation characteristics of plane EM waves with plasma parameters and filament array in a magnetic field, the current density convolution finite difference time-domain method was used. The simulation results show that the decrease in transmittance (peaks) at certain frequencies in the presence of an external magnetic field is obvious, and even at small electron number densities, the transmittance can be reduced with the filament array. In the absence of a magnetic field, the peaks and valleys in the considered frequency bands (f=1~100GHz) are repeated periodically at 30GHz intervals. However, in the presence of a magnetic field, when the layer-to-layer distance is large, they vary to a maximum of 20GHz interval in the f>50GHz band.

Keywords: Femtosecond, Electron number density, Transmittance, Plasma parameters, Circular structure.

1. Introduction

With the rapid development of laser technology, the length of plasma filaments formed in the atmosphere by ultra-short pulse high-intensity lasers can reach hundreds of meters or tens of kilometers. [1-6]

J.Papeer et al. experimentally demonstrated that the plasma filament of a high-density plasma channel generated in the wake of an intense femtosecond pulse propagating in air is sustained for more than 30ns with a free electron density above $10^{15}cm^{-3}$.[7]

Currently, much research on EM wave propagation in such plasma filaments is underway in depth. Yang Liu et al. demonstrated that the doublet-line containing plasma filaments produced by intense femtosecond laser pulses can provide efficient transport of the HPM energy. The attenuation of the HPM in the double line is 0.39dB/m, which is lower than that in the free space.[8] Yu Ren et al. confirmed the microwave guided along double parallel lines of the plasma filament at a distance of about 8cm in the air, and revealed that its structure can support microwave radiation.[9] Through experiments to verify the guiding performance of EM waves in rectangular waveguide, Li Cheng et al. found that the femtosecond laser plasma filament can guide the EM wave with a better performance relative to freely propagating the signal.[10~13]

As the above examples, the study of EM wave

propagation in plasma filaments without magnetic field has been carried out to some extent, but the study of propagation characteristics in the presence of magnetic field has been scarce. The authors simulated a microwave waveguide formed with a high electron number density (10^{21}-10^{22}m^{-3}) under femtosecond multi-terawatt laser systems as three-layer circular plasma channel and studied the propagation characteristics of EM waves in the presence of a magnetic field. Simulating the propagation of plane EM wave in a circular structure by considering even the effect of a magnetic field may be effective in revealing the characteristics of the filament in more detail.

In dispersion and anisotropic media such as magnetized plasma, it is difficult to analyze by the conventional FDTD method. Many methods such as recursive convolution (RC) method [14], auxiliary differential equation (ADE) method [15], Z transformation method [16], current density convolution method [17], and piecewise linear current density RC algorithm [18] were used to simulate the propagation characteristics of EM waves in such a complex dispersion medium. The current density convolution finite difference time domain (JEC-FDTD) method has high computing efficiency and calculation accuracy compared to these methods. [19-21] Therefore, we chose the JEC-FDTD method, which is one of the effective ways to minimize errors in calculation and to save computer memory space. In this paper, the transmission characteristics of EM waves were studied according to the electron number density (N_e =10^{21}~10^{22}m^{-3}), the external magnetic field strength (B=0~4T), and the layer-to-layer distance (d=1.5~4.5mm) in the magnetized filament array with a circular structure.

2. Formulations and Physical model

Consider an isotropic magnetized plasma with collisions. The Maxwell's equations and constitutive relation are given by

$$\nabla \times \boldsymbol{H} = \varepsilon_0 \frac{\partial \boldsymbol{E}}{\partial t} + \boldsymbol{J} \tag{1}$$

$$\nabla \times \boldsymbol{E} = -\mu_0 \frac{\partial \boldsymbol{H}}{\partial t} \tag{2}$$

$$\frac{\mathrm{d}\boldsymbol{J}}{\mathrm{dt}} + \nu \boldsymbol{J} = \varepsilon_0 \omega_p^2 \boldsymbol{E} + \boldsymbol{\omega}_b \times \boldsymbol{J} \tag{3}$$

where $\boldsymbol{E}, \boldsymbol{H}, \boldsymbol{J}, \nu$ and ω_p are the electric field, the magnetic intensity, the polarization current density, the electron collision frequency, and the plasma frequency, respectively.

The electron cyclotron frequency is $\boldsymbol{\omega}_b = q_e \boldsymbol{B}/m_e$, where m_e is the electron mass and q_e is the electron charge.

It is assumed that the y axis is in the direction of external magnetic field, then the x components of (3) becomes

$$\frac{\mathrm{d}J_x}{\mathrm{dt}} + \nu J_x = \varepsilon_0 \omega_p^2 E_x + \omega_b J_z \tag{4}$$

For a time-harmonic dependence, Eq. (4) can be written as

$$J_x(\omega) = \varepsilon_0 \frac{\omega_p^2}{j\omega+\nu} E_x(\omega) + \frac{\omega_b}{j\omega+\nu} J_z(\omega) \tag{5}$$

Taking the inverse Fourier transform (5), we get

$$J_x(t) = \int_0^t \varepsilon_0 \omega_p^2 e^{-\nu(t-\tau)} E_x(\tau)\, d\tau + \int_0^t \omega_b e^{-\nu(t-\tau)} J_z(\tau)\, d\tau \tag{6}$$

If the electric field intensity $\boldsymbol{E}$ is defined at integer time steps, the magnetic field intensity $\boldsymbol{H}$ and the polarization current density $\boldsymbol{J}$ are defined at half integer time steps, respectively, i.e. E^n, $H^{n+1/2}$, and $J^{n+1/2}$. [22, 23]

Using the Yee's notation, $t = (n + 1/2)\Delta t$ and $t = (n - 1/2)\Delta t$ in (6), we have

$$J_x^{n+1/2} = e^{-\nu\left(n+\frac{1}{2}\right)\Delta t}\int_0^{\left(n+\frac{1}{2}\right)\Delta t} e^{\nu\tau}[\,\varepsilon_0\omega_p^2 E(\tau) + \omega_b J_z(\tau)]d\tau \quad (7)$$

$$J_x^{n-1/2} = e^{-\nu\left(n-\frac{1}{2}\right)\Delta t}\int_0^{\left(n-\frac{1}{2}\right)\Delta t} e^{\nu\tau}[\,\varepsilon_0\omega_p^2 E(\tau) + \omega_b J_z(\tau)]d\tau \quad (8)$$

Substituting (8) into (7), we get

$$J_x^{n+1/2} = e^{-\nu\Delta t}J_x^{n-1/2} + e^{-\nu\left(n+\frac{1}{2}\right)\Delta t}\int_{\left(n-\frac{1}{2}\right)\Delta t}^{\left(n+\frac{1}{2}\right)\Delta t} e^{\nu\tau}\,[\varepsilon_0\omega_p^2 E(\tau) + \omega_b J_z(\tau)]d\tau \quad (9)$$

From here, the iterative equation of polarization current density of two-order precision is expressed as

$$J_x^{n+1/2} = e^{-\nu\Delta t}J_x^{n-1/2} + \Delta t e^{-\nu\Delta t/2}[\varepsilon_0\omega_p^2 E_x^n + \omega_b J_z^{n+\frac{1}{2}}] \quad (10)$$

Solving (10) for the x component gives the general form of the FDTD update equation for J_x.

$$J_x\Big|_{i+\frac{1}{2},j,k}^{n+\frac{1}{2}} = e^{-\nu\Delta t}J_x\Big|_{i+\frac{1}{2},j,k}^{n-\frac{1}{2}} + \Delta t e^{-\frac{\nu\Delta t}{2}}[\varepsilon_0\omega_p^2 E_x\Big|_{i+\frac{1}{2},j,k}^{n} + \omega_b J_z\Big|_{i,j,k+\frac{1}{2}}^{n+\frac{1}{2}}] \quad (11)$$

And from (1) and (2), for the x components of $\boldsymbol{E}$ and $\boldsymbol{H}$ can be expressed as [24, 25]

$$H_x\Big|_{i,j+1/2,k+1/2}^{n+1/2} = H_x\Big|_{i,j+1/2,k+1/2}^{n-1/2} + \frac{\Delta t}{\mu_0}\left[\frac{E_y\Big|_{i,j+1/2,k+1}^{n} - E_y\Big|_{i,j+1/2,k}^{n}}{\Delta z} - \frac{E_z\Big|_{i,j+1/2,k+1/2}^{n} - E_z\Big|_{i,j,k+1/2}^{n}}{\Delta y}\right] \quad (12)$$

$$E_x\Big|_{i+1/2,j,k}^{n+1} = E_x\Big|_{i+1/2,j,k}^{n} + \frac{\Delta t}{\epsilon_0}\left[\frac{H_z\Big|_{i+1/2,j+1/2,k}^{n+1/2} - H_z\Big|_{i+1/2,j-1/2,k}^{n+1/2}}{\Delta y} - \frac{H_y\Big|_{i+1/2,j,k+1/2}^{n+1/2} - H_y\Big|_{i+1/2,j,k-1/2}^{n+1/2}}{\Delta z}\right] - J_x\Big|_{i+1/2,j,k}^{n+1/2} \quad (13)$$

We can get the other components of $\boldsymbol{J}$, $\boldsymbol{H}$ and $\boldsymbol{E}$ similarly to Eq. (11)~(13).

The direction of the magnetic field was set perpendicular to the plasma channel (the direction of propagation of EM waves). A linearly polarized plane wave propagating in a direction parallel to the direction of the magnetic field will be decomposed to a right-hand (RH) and a left-hand (LH) circularly polarized wave with different phase velocities.

The calculations results in both cases showed little difference in transmittance due to the relatively high electron number density of filaments. Hence, we consider only the RH circularly polarized wave.

It is assumed that these filaments in each layer are cylindrical and isotropic and the radius of the plasma channel is R=3cm. And the number of layers in the channel is set at 3.

The number of filaments in each layer is N=32 and the filament diameter is 3mm by $r = \pi R/2N$. Therefore, the corresponding array pitch is also about 3mm. Each filament axis is parallel to the z axis and these filaments are alternately arranged along the y axis. In the JEC-FDTD simulation, the time step and the cell size are set as Δt=0.080ps and Δx=Δy=40μm, taking into account the accuracy of calculation and the filament diameter. Each simulation is executed in about 2200-2400 time steps over a relatively long period of time. In order to ensure that the phases of the electric field reaching the outermost layer are the same, the initial phase values of the EM waves are set differently according to each frequency. The collision frequency is set to 10^{12}GHz, and the electron temperature is in the range of 0.2~ 0.4eV depending on the collision frequency and electron number density.

These values are similar to those of the filaments that can actually be made by a femtosecond laser [25, 26].

The electric field intensity E is recorded at a point 14mm from the center of the channel. Here, it

is assumed that the plasma is kept constant by another external power supply and the power of the EM waves is small, so there is no interaction such as plasma generation by the waves.

3. Results and analysis

Fig.1 shows the transmittance of RH polarization wave versus frequency for several values of the external magnetic field strength.

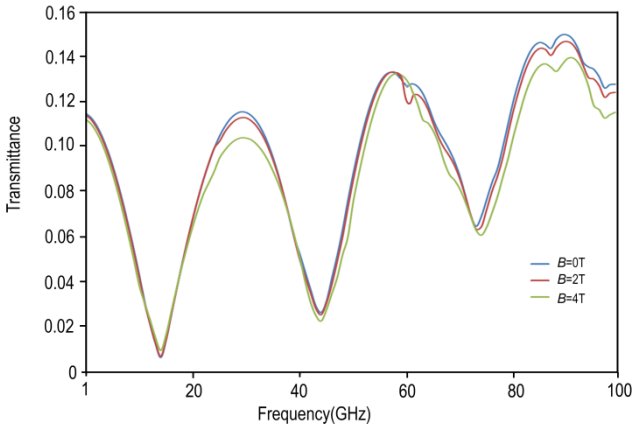

Fig.1. Transmittance of RH polarization wave versus frequency for several values of the external magnetic field strength (N_e=10^{21}m^{-3}, d=0)

As shown in Fig.1, even in the presence of a magnetic field, the peaks and valleys appear periodically at about 30GHz intervals, as in the absence of magnetic field. As the magnetic field strength increases, the transmittance decreases and the peaks and valleys shift to the right. This phenomenon rarely appears in a band with a small frequency (≤50GHz), and it is common only in a band with a large frequency (≥50GHz). When B=2T, the cyclotron resonance absorption, which can be seen in the shape of a small valley, is well visible around 60GHz. These are also in good agreement with the previous literature.[24]

A small valley appears near the frequency of 87GHz. The difference in the path between the two filaments is 1.72mm, which is half of the wavelength (about 3.45mm) corresponding to 87GHz. That is, the interference condition is satisfied and a valley is formed at this frequency.

In the circular array structure, the decrease of the peak and the increase of the attenuation due to the magnetic field are well shown. As the magnetic field strength increases, the transmittance decreases significantly in the peak bands of 25-40GHz and 70-100GHz, and decreases slightly in the valley band. The electrons which vibrate freely in the plasma under a constant external magnetic field move circularly in a plane perpendicular to the magnetic field line at a specific cyclotron frequency. As the magnetic field strength increases, this movement becomes more intense. The directions of the EM waves and movement of these electrons are perpendicular.

That is, it can be seen that the effect of superposition decreases and the transmittance at the peak decreases due to the change of the EM field due to the interaction between the EM wave and electrons. In valleys, there is no such action as above, only attenuation by magnetic field (increased absorption, etc.), so the effect is small. Of course, this attenuation also appears at the peak, but it is relatively smaller than the decrease in the effect of superposition. It is very characteristic that the decrease in transmittance appears strongly only at the first and third peaks and weakly at the second peak when a magnetic field is applied. This is clearly related to the circular

structure and filament array, etc.

According to the calculations, if we change the position of the filaments (i.e. rotate the circular structure by 5.625°), the decrease can only be stronger at the second peak. This means that in this way the superposition can be changed to suit the purpose.

Although the decrease in transmittance is strong only in some specific sections in the figure, the transmittance can be reduced in all bands by increasing the strength of the external magnetic field. For example, when B >4T, the transmittance may decrease by an average of 4% or more in the entire band, and 15% or more in some specific sections. However, if the strength of the external magnetic field is increased, the volume and weight of the device required for this increase, and the problem of reducing it is inevitably raised.

Fig.2 shows the transmittance of RH polarization wave versus frequency for different electron number densities.

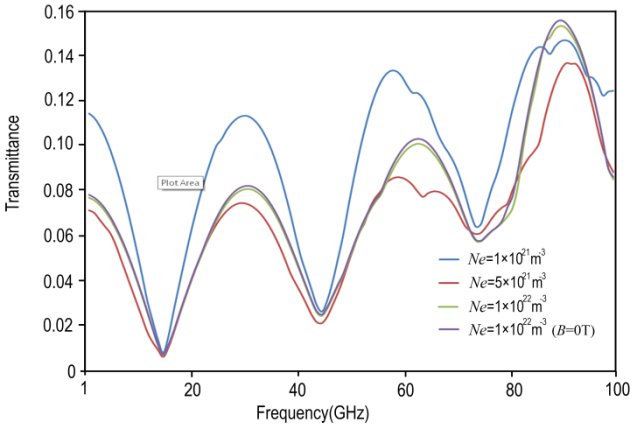

Fig.2. Transmittance of RH polarization wave versus frequency for different electron number densities (B=2T, d=0)

Usually, when the external magnetic field acts, the electron number density decreases. As the external magnetic field strength increases, its decrease becomes more pronounced. Since the electron number density of plasma filaments is large, the decrease in electron number density due to the magnetic field is relatively small. According to the calculation, when $B \leq$2T and the initial electron number density is 10^{21}~10^{22}m^{-3}, the electron number density hardly changes. Therefore, the change in transmittance due to the decrease in electron number density can be negligible. In the figure, as the electron number density increases, the influence of the external magnetic field becomes weaker.

When N_e>10^{21}m^{-3}, the transmission curves with and without a magnetic field are almost the same, and the cyclotron resonance absorption at 60GHz is also almost non-existent. And when N_e =10^{22}m^{-3}, the decrease that appeared at 60GHz and 87GHz as seen above also disappears. It can be considered that as the electron number density increases, the distance between charged particles decreases, and thus the electric force between them increases, and thus the influence of the external magnetic field appears small. In the figure, as in the previous literature, the transmittance decreases as the electron number density increases.[13]

As the plasma density increases, the number of electrons in the plasma increases, and the probability of collision between the incident EM waves and charged particles increases. The electron absorbs more energy from the incident EM wave, thereby accelerating its irregular motion. Thus, the absorptance increases and the transmittance decreases. However, when N_e =0.5×10^{22}m^{-3}, the transmittance is small compared to 10^{22}m^{-3} in a wide

band.

This is also related to the structure of the plasma filament layer. The skin layer depth depends on the electron number density, and the superposition of transmitted waves appears differently accordingly. That is, if the parameters of the filament layer are well selected, the same transmission characteristics as in the high electron density even at low electron density can be obtained.

Fig.3 shows the transmittance versus frequency for several values of the layer-to-layer distance (d) in the external magnetic field.

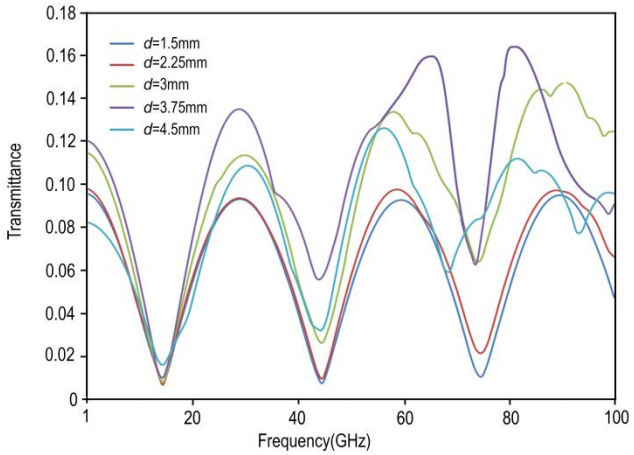

Fig.3. Transmittance versus frequency for several values of d in the external magnetic field (N_e=10^{21}m^{-3}, B=2T)

The transmission of EM waves according to the layer-to-layer distance is relatively complex. Usually, as the layer-to-layer distance increases, the transmittance increases. When d <3mm, the transmission characteristics are almost the same. In the case of d≥3mm, the change in transmittance according to the layer-to-layer distance is relatively large. When d=3.75mm, the transmittance is the largest in the entire region. In this case, the transmittance in the band of f>20GHz is about 30% larger than when d=3mm and 4.5mm. It can be considered that as d increases, the propagation passage between the filaments increases, so that refraction, reflection and absorption become small. And it shows that d≈3.8mm is a reasonable value to obtain high transmittance for a wide frequency band in a given filament layer structure.

If d is too large, the propagation passage becomes large, but the difference in the path is changed accordingly, so that the overlap condition according to different frequencies is not satisfied, and the transmittance may be reduced (d=4.5mm). The feature in the figure is the decrease of the peak spacing with frequency. This is well observed in the band above 50GHz for d≥3.75mm. In the case of d ≤3mm, the frequency interval between two adjacent peaks is about 30GHz. However, when d≥3.75mm, this frequency interval is about 20GHz.

This indicates that the suitable choice of the parameters of the circular plasma filament layer in the presence of a magnetic field can optimally adjust the peak-to-peak interval.

4. Conclusion

Here, we investigated the propagation characteristics of RH polarized waves in magnetized plasma filament layer with a multilayer circular structure. When an external magnetic field is applied, for a given circular structure, the transmittance decreases significantly at the first and third peaks and slightly decreases at the second peak.

That is, the peak appears periodically at 30GHz intervals, but the variation of transmittance reduction is well at 60GHz intervals.

The opposite effect can be achieved by rotating

the layer structure by a certain angle when the propagation direction is constant. The greater the electron number density, the weaker the influence of the external magnetic field, and even when the electron number density is relatively small, a large transmittance can be obtained by adjusting the array parameters. A small layer-to-layer distance gives a similar transmission property to that without a magnetic field. However, when the layer-to-layer distance is large, the transmittance increases a lot and the peak spacing decreases.

Funding

The authors did not receive any fund to perform this work.

Conflicts of interest

The authors of this paper have no conflict of interest.

Author contribution statement

Un-Ha Kim: Conceptualization, Methodology, Software. In-Ho Pak: Data curation, Writing - original draft, Visualization, Investigation, Supervision. Su-Hyang Pak: Software, Validation, Writing - review & editing. Yong-Jun Kim: Validation, Writing - review & editing.

References

[1] Tzortzakis S.; Prade B.; Franco M.; Mysyrowicz A.; Huller S. 2001- **Femtosecond laser-guided electric discharge in air.** Phys Rev E Stat Nonlin Soft Matter Phys. 64,

057401.https://doi.org/10.1103/PhysRevE.64.057401

[2] Bodrov SB.; Kulagin DI.; Malkov YA.; Murzanev AA. 2012- **Initiation and channelling of a microwave discharge by a plasma filament created in atmospheric air by an intense femtosecond laser pulse.** Journal of Physics D. Applied Physics. 45**.** 04520

. https://doi.org/10.1088/0022-3727/45/4/045202

[3] Kaleris K.; Orfanos. Y.; Bakarezos M. 2019 -**Experimental and analytical evaluation of the acoustic radiation of femtosecond laser plasma filament sound sources in air.** J Acoust Soc Am**.** 146. EL212. https://doi.org/10.1121/1.5124509

[4] Liu.; Weiwei.; Lin.; Lie.; 2023- **Manipulation of Long-Distance femtosecond laser Filamentation: From physical model to acoustic diagnosis.** Elsevier Ltd. 157**.**

https://doi.org/10.1016/j.optlastec.2022.108636

[5] Li D.; Yan B.; Yuan Y. 2024 - **Real-Time Demonstration of Multi-Gigabit/s Free-Space Optical Communications Employing Femtosecond Laser Filaments in Complex Environment.** IEEE. 42. 13. https://doi.org/10.1109/JLT.2024.3375121

[6] Zemlyanov, A.; Geints. 2021- **Numerical Simulation of Filamentation of Synthesized Femtosecond Profile Laser Beams in Air**. Springer. 34**.** 6.

https://doi.org/10.1134/S1024856021060105

[7] Papeer J.; Botton M. 2014- **Extended lifetime of high density plasma filament generated by a dual femtosecond-nanosecond laser pulse in air.** New Journal of Physics**.** 16.123046 .

https://doi.org/10.1088/1367-2360/16/12/123046

[8] Liu Y.; Chen Z.; Shi J. 2019- **Simulation of HPM Propagation in a Double-Line Containing Plasma Filaments Produced by Intense Femtosecond Laser Pulses.** IEEE Transactions on Plasma Science**.** 47, 1394. https://doi.org/10.1109/TPS.2018.2887231

[9] Ren Y.; Alshershby M.; Hao Z.; Zhao Z.; Lin J. 2013- **Microwave guiding along**

double femtosecond filaments in air. PHYSICAL REVIEW E. 88. 013104.

https://doi.org/10.1103/PhysRevE.88.013104

[10]Ren Y.; Alshershby M.; Qin J.; Hao Z.; Lin J. 2013- **Microwave guiding in air along single femtosecond laser filament.** Journal of Applied Physics. 113**.** 094904

https://doi.org/10.1063/1.4794518

[11]Liu Y.; Chen Z.; Cheng L.; Sun K .; Shi J. 2020- **6 GHz electromagnetic wave guiding along a femtosecond laser plasma filament.** Microwave and Optical Technology Letters. 62. 1009–16.

https://doi.org/10.1002/mop.32140

[12]Liu Y.; Cheng L.; Dou X.; Chen W.; Hu Y.; Shi J. 2020- **Guiding performance of 6 GHz electromagnetic wave by single laser plasma filament.** Laser Physics Letters. 17. https://doi.org/10.1088/1612-202X/ab60ae

[13]Dormidonov A.E.; Valuev V.V. 2007 **-Laser Filament Induced Microwave Waveguide in Air**. Proc. of SPIE. Vol.6733. 67332S-1. https://doi.org/10.1117/12.753246

[14]Kelley DF.; Luebbers RJ .1996- **Piecewise Linear Recursive Convolution for Dispersive Media Using FDTD** IEEE Transactions on Antennas and Propagation. 44, 792-7 .https://doi.org/10.1109/8.509882

[15]Ding J.; Yang Y .; Zhao Z. 2017- **Optimized ADE-FDTD Method in Unmagnetized Plasma**. IEEE 2nd Information Technology, Networking, Electronic and Automation Control Conference (ITNEC), 1110-2 .https://doi.org/10.1109/ITNEC.2017.8284947

[16]Nayyeri V.; Soleimani M.; Rashed Mohassel.; Dehmollaian M. 2011- **FDTD Modeling of Dispersive Bianisotropic Media Using Z-Transform Method**. IEEE Transactions on Antennas and Propagation. 59. 2268-79.

https://doi.org/10.1109/tap.2011.2143677

[17]Liu S.; Liu M.; Hong W. 2008 - **Modified piecewise linear current density recursive convolution finite-difference time-domain method for anisotropic magnetised plasmas.** IET Microwaves, Antennas & Propagation. 2, 677-85. https://doi.org/10.1049/iet-map:20070291

[18]Chen B.K. 2015- **A Novel Piecewise Linear Recursive Convolution Approach for Lorentz media Using the ADE- FDTD Method**. Proceedings of the 3rd International Conference on Mechatronics and Industrial Informatics. 761-5. https://doi.org/10.2991/icmii-15.2015.132

[19]Song D.J.; Yang H.W.; Wang G.B. 2016- **A research for plasma electromagnetic character using JEC-CN-FDTD algorithm based on ICCG method.** Optik. 127, 1121–5 .https://doi.org/10.1016/j.ijleo.2015.10.139

[20]Song D.J.; Yang Z.K.; Liu Y.J.; Niu Q-X.; Yang H-W .2015- **A Study on Plasma Photonic Crystals: Electromagnetic Characteristics Using ICCG-based JEC-CN-FDTD Algorithm**. Zeitschrift für Naturforschung A. 70,881-8. https://doi.org/10.1515/zna-2015-0279

[21]Liu J.; Yan Z.; Ji J.; Chang Q.; Song H. 2020- **Study on Tunable Magnetized Plasma Frequency Selective Surface Using JEC-FDTD Method**. IEEE TRANSACTIONS ON PLASMA SCIENCE. 48, 3479-86. https://doi.org/10.1109/TPS.2020.3020150

[22]Yu Y.; Niu J.; Simpson J.J. 2012 -**A 3-D Global Earth-Ionosphere FDTD Model Including an Anisotropic Magnetized Plasma Ionosphere**. IEEE Transactions on Antennas and Propagation. 60, 3246-56. https://doi.org/10.1109/tap.2012.2196937

[23]Xu L.; Yuan N .2005- **JEC-FDTD for 2-D Conducting Cylinder Coated by Anisotropic Magnetized Plasma.** IEEE

MICROWAVE AND WIRELESS COMPONENTS LETTERS. 15. 892-5.https://doi.org/10.1109/LMWC.2005.859970

[24]Nguyen B.T.; Samimi A.; Vergara S.W.; Sarris C.D.; Simpson J.J. 2019-**Analysis of Electromagnetic Wave Propagation in Variable Magnetized Plasma via Polynomial Chaos Expansion**. IEEE TRANSACTIONS ON ANTENNAS AND PROPAGATION. 67, 438-49 .https://doi.org/10.1109/TAP.2018.2879676

[25]Dormidonov A.E.; Valuev V.V.; Dmitriev V.L.; Shlenov S.A. Kandidov V.P. 2007 -**Laser Filament Induced Microwave Waveguide in Air**. Proc. SPIE, International Conference on Lasers, Applications, and Technologies: Environmental Monitoring and Ecological Applications; Optical Sensors in Biological, Chemical, and Engineering Technologies; and Femtosecond Laser Pulse Filamentation**.** 6733. 67332S. https://doi.org/10.1117/12.753246

[26]Sun Z.; Chen J.; Rudolph W. 2011-**Determination of the transient electron temperature in a femtosecond-laser-induced air plasma filament**. Phys Rev E Stat Nonlin Soft Matter Phys. 83.046408 .https://doi.org/10.1103/PhysRevE.83.046408